

Submillimeter spectroscopy of semiconductors

E. M. Gershenzon, G. N. Gol'tsman, and N. G. Ptitsina

Moscow State Pedagogical Institute

(Submitted 15 September 1972)

Zh. Eksp. Teor. Fiz. 64, 587-598 (February 1973)

The possibility is considered of carrying out submillimeter-wave spectral investigations of semiconductors by means of a high resolution spectrometer with backward-wave tubes. Results of a study of the excitation spectra of small impurities, $D^-(A^+)$ centers and free excitons in germanium are presented.

1. INTRODUCTION

The 100–1000 μ electromagnetic wave band is of considerable interest in semiconductor research. It suffices to state that practically the entire excited-state spectrum of shallow impurities in semiconductors lies in this band, which includes the characteristic frequencies of exciton transitions, of $D^-(A^+)$ centers produced when an extra electron (hole) attaches itself to a neutral impurity atom, and Zeeman and Stark transitions for excited states of the impurities; it is possible to realize in this band quantum cyclotron and electron paramagnetic resonances, cyclotron resonance of electrons localized on impurities, etc. In spite of the great promise offered by research in this frequency band, this research is only at the initial stage at present. The primary difficulties are technical, since this region of the electromagnetic spectrum lies at the junction between bands handled by optical and radio means. Much progress has been made of late in the development of radiation sources and receivers, in the guidance of the radiation, in the measurement techniques, etc.

The principal methods in the spectroscopy of semiconductors at submillimeter wavelengths are presently optical, using the emission of a thermal or gas-discharge source, spectral resolution with the aid of diffraction gratings (usually echelettes), or Fourier transformation of the spectrum. The available spectrometers have low sensitivity and poor resolution. Submillimeter lasers with monochromaticity and power level sufficient to provide high resolution and sensitivity are in practice not tunable and make it possible to perform measurements only at fixed frequencies, with variation of the magnetic field or of other parameters, thus limiting the research possibilities.

A new possibility exists now for spectral investigations. Recently developed submillimeter microwave generators with backward-wave tubes (BWT)^[1] deliver monochromatic radiation of power $\sim 10^{-3}$ W and can be tuned in a wide frequency range by varying the supply voltage. A shortcoming of BWT is the choppy character of their amplitude-frequency characteristics. However, the advantages of BWT spectrometers over the customarily employed optical long-wave IR receiver, namely the increase of resolution to $\sim 10^{-4}$ cm^{-1} and an increase by more than four orders of magnitude in the sensitivity, make it possible to investigate many new problems.

The present article is devoted to a study of photoconductivity and absorption in semiconductors such as Ge and GaAs at submillimeter wavelengths, using BWT.

2. APPARATUS

To investigate the behavior of semiconductors at submillimeter wavelengths we used a spectrometer covering the spectral range from 2.0 to 0.25 mm with the aid of several BWT^[2,3]. The main problem in developing such a spectrometer is stabilization of the radiation power incident on the investigated sample in the entire range of the tunable frequency of each BWT, in spite of the choppy character of its amplitude-frequency characteristic.

We have developed a simple stabilization method^[3] wherein the variation of the radiation power level does not exceed 2–3% when the generated power changes by 10–15 dB.

Figure 1 shows a block diagram of the spectrometer developed for use at low temperatures. The radiation-power level is equalized with the aid of an attenuator connected in an electromechanical negative-feedback loop consisting of a narrow band amplifier (LFA), a synchronous detector (SD), a dc amplifier (DCA), and an electric motor (EM) coupled to the attenuator by a reduction gear. The DWT radiation travels through a quasi-optical channel to the investigated sample and to an n-InSb detector, which are situated under identical conditions; the walls of the channel and of the chambers with the samples are made of a material of a radiation-absorbing material to prevent secondary reflections. The mechanical chopper (MC), which modulates the radiation in the spectrometer, produces a low-frequency voltage proportional to the incident power, which is picked off the n-In-Sb receiver and fed to the synchronous detector. The reference voltage for the SD is generated by the same chopper. The attenuator setting is such that it introduces no damping at the lowest generated power in the tuning range of the BWT (~ 100 μ W); the SW setting is such that in this case the output voltage of the DCA is zero. In this case, any change of the power level produced by tuning the BWT causes the motor (and hence the attenuator) to rotate until the previous power level is restored at the sample.

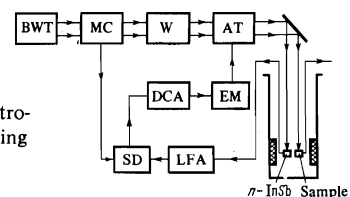


FIG. 1. Block diagram of spectrometer. W—wave meter, the remaining symbols are defined in the text.

The spectrometer measurements are based either on the photoconductivity of the investigated sample or on the absorption of radiation by the n-InSb receiver located behind the sample. If the absorption of the submillimeter radiation by the sample is small, then the high-frequency power modulation customarily employed to produce synchronous detection is replaced by a balanced indication, wherein the coefficient of absorption of radiation by the sample is modulated (by varying the carrier density with the aid of additional illumination, by varying the magnetic field, etc.), the signal is picked off the contact of the n-InSb detector, and the stabilization circuit eliminates the deviations by varying the dc voltage, amplified directly by the DCA, across the same contacts. This stabilization method is less efficient than the previously described one, but is useful in the measurements.

The sample holder is placed in a helium cryostat with a superconducting solenoid, and provision is made for applying additional illumination on the sample. The investigations were performed at temperatures $T = 1.6-12^\circ\text{K}$ and in magnetic fields $H = 0-50\text{ kOe}$.

3. STUDY OF EXCITED STATES OF IMPURITIES IN SEMICONDUCTORS

The detailed study of the energy structure of excited states of shallow impurities in semiconductors has evoked considerable interest of late. The theoretical analysis is usually carried out in the effective-mass approximation by a variational method^[4,5].

The spectrum of the excited states of the donors in Ge and Si and some other semiconductors was calculated using almost-hydrogenlike wave functions as the trial functions. In such an approach, the hydrogen quantum numbers n , l , and m (principal, orbital, and magnetic) are used, and the corresponding series of levels are determined in the Coulomb-potential approximation with the crystal band structure taken into account. The shortcomings of such an analysis are obvious: no account is taken of the individual nature of the impurities or of the difference between the impurity-atom potential and the Coulomb potential near the nucleus; this leads to particular inaccuracies in the determination of the states of the ns series; considerable difficulties are encountered in the calculation of the acceptor states, etc. Experiment therefore becomes of special significance, all the more since many series of energy levels have not been calculated at all even for the donors in Ge and Si (for example, the series $nd_{\pm 1}$, $ng_{\pm 1}$).

The widths of the spectral lines corresponding to transitions between impurity states were also investigated theoretically^[6,7]. At low concentration of the impurities and defects, it should be determined by the interaction of the bound electrons with the phonons, and with increasing impurity concentration, the interaction of the bound electrons with each other comes into play. Also leading to the broadening of the lines is the growth of the number of ionized impurity centers, which produce strong random internal electric fields that split the energy levels of the bound electrons (the Stark effect) and increase the defect concentration in the material.

A number of theoretical results have by now been compared with experiment. The measurements were made by long-wave IR spectroscopy methods. The registered quantity was either the radiation absorption that causes the transitions from the ground state of the impurity to the excited states (for example^[8]), or the

change in conductivity when such transitions are accompanied by thermal transfer of electrons to the conduction band^[9].

We have investigated the photoconductivity of n-GaAs and Ge in the wavelength range $2-0.25\text{ mm}$. Unlike in other investigations^[8-13], we registered transitions not only from the ground state of the impurity to the excited state, but also between excited states with subsequent thermal transfer to the free band (photothermal ionization of excited states^[2]). Such transitions could not be observed in Ge by the method of long-wave IR spectroscopy, since the absorption coefficient in this case is smaller by 3-5 orders of magnitude, owing to the small population of the excited states even at $T \sim 7 = 10^\circ\text{K}$, and the sensitivity of the spectrometers is low. Unfortunately, the short-wave limit of our spectrometer did not make it possible to observe transitions from the ground state of the impurity in Ge, and we were able to observe only transitions between excited states. In GaAs, the entire spectrum of the shallow donors lies in the investigated band.

The present article is devoted mainly to the investigation of Ge. Data on GeAs are given to demonstrate that the study of the same states with and without the use of transitions from the ground state, yields the same information. Figure 2 shows by way of example the photoconductivity spectra of GaAs ($\Delta\sigma$ is the change of conductivity of the sample) with an impurity density difference $N_d - N_a = 6 \times 10^{13}\text{ cm}^{-3}$ and electron mobility at 77°K equal to $\mu_{77^\circ} = 135 \times 10^3\text{ cm}^2/\text{V-sec}$, at wavelengths $774\text{ }\mu$ (Fig. 2a) and $256\text{ }\mu$ (Fig. 2b), as functions of the magnetic field. On the first of these figures we see transitions from the ground state 1s to the excited states $2p_{+1}$ (I) and $2p_0$ (II), which were observed also by others^[11-13], one of the transition lines between excited states (1), and the electron cyclotron-resonance peak (CR). The other shows lines corresponding to the transitions $2p_{-1} \rightarrow 2p_0$ (6), $2s \rightarrow 2p_{+1}$ (3), $2p_{-1} \rightarrow 2s$ (4), and others. The line intensities can be compared with the aid of the CR. If the presented spectra are used to determine the energies of the excited states and the line width for transitions to one and the same state from the ground state or from an excited state, then the results coincide. The equality of the line widths, in particular, is evidence that the width is determined by the excited state.

The GaAs available to us had an appreciable impurity density, and therefore narrow impurity-transition lines were obtained only in sufficiently strong magnetic fields when the impurities were neutralized by the interband light. A study of the influence of a strong magnetic field

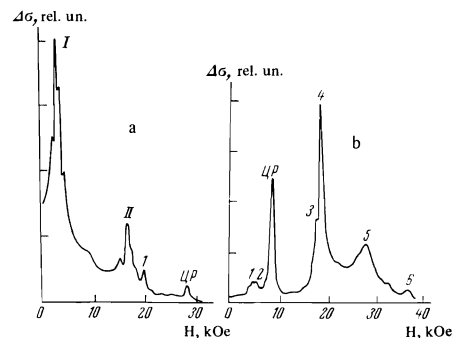


FIG. 2. Photoconductivity spectra ($\Delta\sigma$ is the change of conductivity) of GaAs at $T = 1.6^\circ\text{K}$: a) $\lambda = 774\text{ }\mu$, b) $\lambda = 256\text{ }\mu$.

is beyond the scope of the present article. The results of the study of the spectrum in GaAs was considered by us separately^[14]. We shall henceforth deal mainly with Ge, where a maximum impurity concentration $N_d + N_a \lesssim 10^{12} \text{ cm}^{-3}$ was reached.

Figure 3 shows sections of the photoconductivity spectrum at $T = 7^\circ \text{ K}$ for a Ge sample with donor concentration $N_d = 2 \times 10^{13} \text{ cm}^{-3}$ (Sb) and acceptor concentration $N_a = 2 \times 10^{12} \text{ cm}^{-3}$. The abscissas represent the energy ϵ of the incident photon (λ is its wavelength). The table contains a complete list of the transition energies observed in Ge doped with Sb.

All the spectral lines in Ge samples with different Sb concentrations correspond to the same energy values. For samples doped with P and As, the spectra differ somewhat from the spectrum of Sb in Ge, namely, lines with energy 3.50 meV and higher (Sb) are shifted towards lower energies by an amount 0.02 meV for P and 0.03 meV for As. The remaining intense lines have the same spectral positions for Sb, P, and As. The spectral line width changes from 0.008 to 0.02 meV for different lines at $N_d \sim 10^{13} \text{ cm}^{-3}$, and for some of them it does not become any narrower with further decrease of the impurity concentration.

The photoconductivity spectral lines have high intensity and different lines have different temperature dependences; namely, when the temperature is increased from 4.2° K the value of $\Delta\sigma$ increases by a factor 10^2-10^3 and reaches saturation when $T = 9-10^\circ \text{ K}$ is reached. By then, the line width is also much larger, although it changes little up to $7-8^\circ \text{ K}$.

Figure 4 shows the level scheme of the donors (Sb) in Ge. In the center are shown the values calculated in the effective-mass approximation^[5], on the left are shown the optical transitions from the ground state to excited states^[8] (only transitions from the triply degenerate ground state of the impurity are shown), and on the right side are shown some of the transitions observed by us.

We see that the IR spectroscopy methods shows only the p-states of the donors, to which sufficiently intense

N_d	ϵ of lines, meV	$\epsilon_n - \epsilon_m$, meV	Identification of lines	N_d	ϵ of lines, meV	$\epsilon_n - \epsilon_m$, meV	Identification of lines
1	0.60	1.34-0.73	$3d_0 \rightarrow 4p_{\pm 1}$	12	1.34	2.06-0.73	$3s \rightarrow 4p_{\pm 1}$
2	0.68	—	—	13	1.40	—	—
3	0.71	1.34-0.63	$3d_0 \rightarrow c$	14	1.41	—	—
4	0.73	1.34-0.61	$3d_0 \rightarrow 4f_{\pm 1}$	15	1.45	2.06-0.61	$3s \rightarrow 4f_{\pm 1}$
5	0.82	1.67-0.85	$4p_0 \rightarrow b$	16	1.57	—	—
6	0.90	—	—	17	1.87	3.60-1.73	$2s \rightarrow 2p_{\pm 1}$
7	1.04	1.67-0.63	$4p_0 \rightarrow c$	18	3.02	4.75-1.73	$2p_0 \rightarrow 2p_{\pm 1}$
8	1.11	—	—	19	3.50	4.75-1.25	$2p_0 \rightarrow a$
9	1.16	4.75-3.60	$2p_0 \rightarrow 2s$	20	3.90	4.75-0.85	$2p_0 \rightarrow b$
10	1.22	2.06-0.85	$3s \rightarrow b$	21	4.12	4.75-0.63	$2p_0 \rightarrow c$
11	1.31	2.56-1.25	$3p_0 \rightarrow a$	22	4.24	4.75-0.51	$2p_0 \rightarrow d$

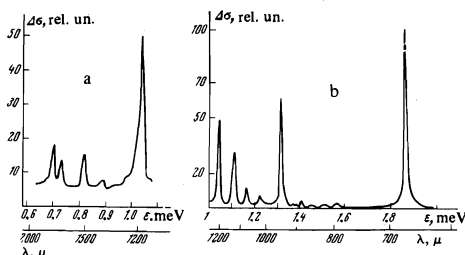


FIG. 3. Photoconductivity spectra of Ge doped with Sb at $T \sim 8^\circ \text{ K}$: a) $\lambda = 2000-1200 \mu$, b) $\lambda = 1200-600 \mu$.

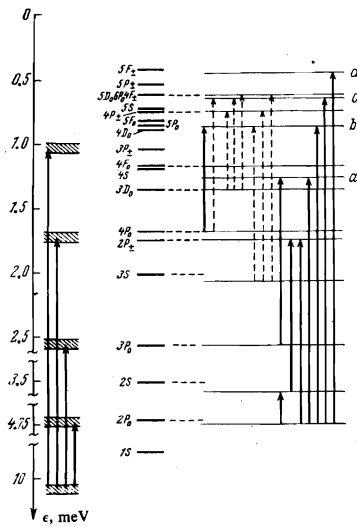


FIG. 4. Level scheme of the states of the donors in Ge.

transitions from the ground state occur. The experimentally obtained values of the p-states agree well with the theoretical ones. The spectral line width is not less than 0.06 meV and is governed by the lifetime of the electrons in the excited states^[15], although this value is close to the resolution limit of the spectrometer. The shaded energy interval in Fig. 4 is equal to this value, 0.06 meV.

The BWT spectrometer reveals more lines, but these lines cannot be drawn in the figure to scale.

Identification of the lines investigated by us encounters significant difficulties. The reason is that energy levels which have previously not been observed experimentally take part in practically each of the transitions. Indeed, we observed only excited p-states, the optical transitions between which should be of low intensity. The solid arrows in the right-hand side of Fig. 4 show the transitions which, in our opinion, have been reliably determined; the dashed arrows represent the proposed identification, which is also used in the table. To interpret the lines it is necessary, besides knowing their energy position, to use data on the Zeeman effect, on the broadening that follows the increase in the density of the main impurity, and on the difference between the Sb, P, and As spectra.

By way of example, we present an identification of the four spectral lines 1.16, 1.31, 1.87, and 3.50 meV. The line 1.16 meV corresponds to the $2p_0 \rightarrow 2s$ transition, and 1.87 corresponds to $2s \rightarrow 2p_{\pm 1}$. This follows from the fact that the sum of the energies of these lines is 3.03 meV, while the sum of the transition energies is equal to the energy difference between the levels $2p_0$ and $2p_{\pm 1}$, the measured value of which^[16] is 3.03 ± 0.02 meV. The transition between the states $2p_0$ and $2p$ was observed in our experiments directly and its energy amounted to 3.02 meV; as expected, the corresponding line is of low intensity.

Calculation of the ionization of the 2s level yields a value 3.52 meV^[5]. Our experimental data give 3.60 meV. It is interesting that this value is independent of the type of impurity. It follows therefore that either the 2s state is not split into a singlet and triplet in the case of all three donors (unlike the ground state 1s), or that we have observed transitions only from the triplet state, the energy of which depends little on the type of impurity even in the case of the 1s state.

In the case of the two other lines, the 3.50 meV and 1.31 meV correspond to the transitions $2p_0 \rightarrow 3d_{z_1}$ and $3p_0 \rightarrow 3d_{z_1}$. Indeed, the energy of the first of these lines is so large, that the initial state for it is the first excited state of $2p_0$, and the energy difference between these lines is 2.19 meV, which agrees well with the Japanese measurements^[16]: $2p_0 - 3p_0 = 2.20 \pm 0.02$ meV. The energy of the $3d_{z_1}$ state, which has never been calculated before and apparently never been observed experimentally, turns out to be 1.25 meV. This state and the three other states whose energies were determined by us experimentally are apparently not all d-type states, but a check on this fact calls for a theoretical calculation. The depths of the state $2p_0$ for Sb, P, and As were determined experimentally with an accuracy better by one order of magnitude than heretofore, and it was found that these values differ noticeably.

This identification of the lines is confirmed by their behavior in a magnetic field: the 1.16 meV line, unlike the 1.87, 1.31, and 3.50 meV lines, is split. The very fact of splitting, and also its singularities in a strong magnetic field, allow us to state that the first transition occurs without change in the magnetic quantum number, in the second two the principal number remains unchanged but the magnetic number changes by ± 1 , and in the fourth term the principal number changes by one and the magnetic number by ± 1 . The identification likewise does not contradict the concentration broadening of the lines: these lines do not broaden noticeably at concentrations up to 2×10^{14} cm⁻³, and therefore correspond to sufficiently low-lying excited states.

Figures 5 and 6 illustrate the possibilities of measuring the Zeeman effect of the excited states of impurities at submillimeter wavelengths. Figure 5 shows the splitting of part of the spectral lines in a magnetic field up to 45 kOe (only some of the branches are shown, so as not to clutter up the figure). We see that the behavior of the spectral lines in the magnetic field is not uniform. This fact yields definite information for line identification. In particular, the linearity of the splitting of the 1.31 and 1.27 meV lines^[17] up to strong magnetic fields H indicates that these transitions occur without a change in the principal quantum number, for in this case there is practically no quadratic level shift in a magnetic field. Unlike these two lines, the lower branch of the 3.50 meV line becomes less steep at $H \sim 17$ kOe, and the 1.04 line becomes less steep at ~ 4 kOe.

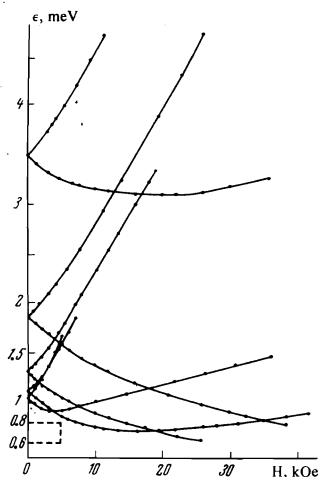


FIG. 5. Dependence of the transition energy ϵ of the lines 1.04, 1.11, 1.31, 1.87, and 3.50 meV on the magnetic field in Ge (Sb) ($H \parallel [111]$).

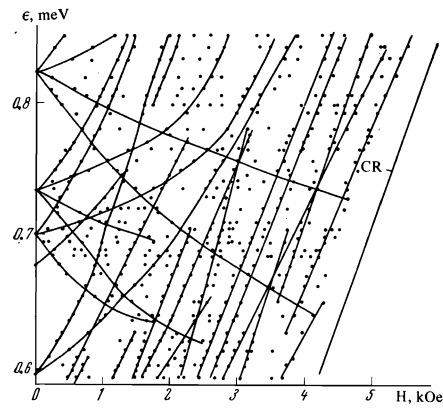


FIG. 6. Total of spectrum of the transition energies observed in the range $\epsilon = 0.6-0.85$ meV following a magnetic-field variation $H = 0-5$ kOe ($H \parallel [111]$) (the region in the dashed rectangle of Fig. 5).

The dashed rectangle of Fig. 5 is shown in a different scale in Fig. 6. We see that the abundance of lines makes these measurements much more interesting than in the infrared technology. We note that an investigation of the Zeeman effect at larger wavelengths ($\lambda \gtrsim 2$ mm) makes it possible to study even higher excited states of donors in Ge.

4. POSSIBILITIES OF INVESTIGATING IMPURITY STATES BY ADDITIONAL ILLUMINATION

Additional opportunities of studying impurities at submillimeter wavelengths are obtained by illuminating the sample with interband light. Generation of electrons and holes can lead to a significant change in the population of the impurity states, to the formation of new complexes, and to other effects. We shall discuss two manifestations of the influence of additional illumination on the impurity states.

A. Minority impurities. Under dark conditions, the minority impurities are fully ionized. Therefore in the case of n-Ge the observed spectral of Fig. 4 belong only to shallow donors. Additional illumination leads to neutralization of the impurities and to a possibility of indicating spectral lines corresponding to a compensating shallow impurity.

We have performed these experiments with both n-Ge and p-Ge. Figure 7 shows schematically the spectral photoconductivity lines for n- and p-type samples in the absence of special additional illumination and following illumination with interband light. Figure 8 shows a section of the photoconductivity spectrum of a p-Ge sample with $N_a = 2 \times 10^{12}$ cm⁻³ and $N_d = 2 \times 10^{11}$ cm⁻³ at $T = 5^\circ$ K under illumination conditions. We see that the photoresponses corresponding to the main and compensating impurities have opposite signs, with negative photoconductivity corresponding to excitation of the compensating impurity. The decrease of the conductivity is apparently due to the decrease in the lifetime of the majority carriers, and consequently to the decrease of their concentration as a result of the appearance of minority carriers following photothermal ionization of the compensating impurity.

It is evident from Fig. 8 that the most intense lines of the minority impurity are perfectly well observed in the spectrum even at 10% compensation. They can be measured down to $\sim 1\%$ compensation, i.e., at a concentration $\sim 10^{10}$ cm⁻³. Thus, measurements with additional

illumination have made it possible to determine the relative concentrations of the donors and acceptors in the sample and to obtain a chemical analysis of the shallow impurities even in extremely purified Ge, by using the spectral-line positions. In particular, the compensating impurity in the sample of Fig. 8 was phosphorus.

A similar procedure of investigating the compensating impurities was used by us in the study of the defect-formation processes in Ge bombarded with γ quanta^[18].

B. $D^-(A^+)$ centers. When one more electron is added to a neutral donor (or one extra hole to an acceptor) in a semiconductor, so-called D^- and A^- centers are produced. Their ionization energy lies in the submillimeter wave band^[19,20]. Spectral investigations performed at sufficiently low temperatures ($kT \ll \epsilon_i$) can therefore be used to determine the long-wave photoconductivity limit, and by the same token to determine the values of ϵ_i for different impurities and perform other investigations of such centers. Additional information concerning these centers is obtained by studying the absorption of submillimeter radiation. In these experiments, additional illumination is necessary to produce the concentration of neutral impurities and free carriers needed for the formation of the $D^-(A^+)$ centers even in strongly compensated samples.

The photoconductivity produced when $D^-(A^+)$ centers are ionized in Ge was investigated by us earlier^[10]. In the present study we investigated also the absorption, which reached $\sim 10\%$ in our experiments.

The photoconductivity and absorption spectra turned out to be similar and gave identical values of ϵ_i . By way of example, Fig. 9 shows the photoconductivity spectrum ($\Delta\sigma$) of a Ge (As) sample ($N_d = 5 \times 10^{14} \text{ cm}^{-3}$, $N_a = 10^{13} \text{ cm}^{-3}$) at $T = 1.5^\circ \text{K}$; ϵ_i amounts to 1.55 meV.

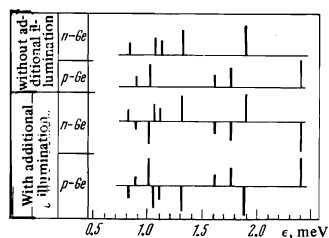


FIG. 7. Diagram of photoconductivity spectra of Ge samples following interband illumination.

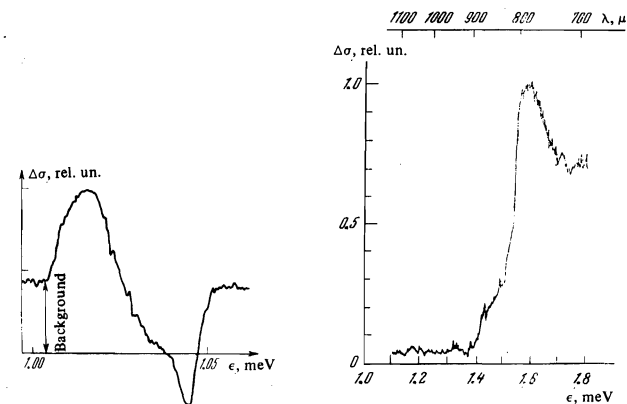


FIG. 8

FIG. 8. Photoconductivity spectrum of p-Ge sample (interband illumination, $\epsilon = 1.00\text{--}1.05 \text{ meV}$, $T \sim 5^\circ \text{K}$).

FIG. 9. Photoconductivity spectrum of Ge(As) with $N_d = 5 \times 10^{14} \text{ cm}^{-3}$, $N_a = 10^{13} \text{ cm}^{-3}$ (interband illumination $\lambda = 1.1\text{--}0.7 \text{ mm}$, $T \sim 1.6^\circ \text{K}$).

An increase of the As concentration to $2 \times 10^{16} \text{ cm}^{-3}$ produces practically no change in the absorption and photoconductivity spectra. At higher concentrations, the long-wave boundary of the spectrum becomes blurred and the singularities of the spectra disappear completely at $N_{As} \sim 7 \times 10^{16}$. It follows therefore that the radius of the bound state in such a center is $\sim 150 \text{ \AA}$ if the interaction between D^- centers is assumed to be significant at $2r \approx N_{As}^{-1/3}$ ^[20].

Other impurities, including acceptors, were also investigated^[19].

The aggregate of the experiments on the $D^-(A^+)$ centers (primarily, such data as the absence of fine structure in the spectra and the small radius of the bound state) apparently indicate that these centers are characterized by the presence of only one forbidden-band energy level that depends on the nature of the impurity.

5. POSSIBILITIES OF EXCITON INVESTIGATION

The investigation of excitons in many semiconductors is of particular interest at submillimeter wavelengths, since this band corresponds to the characteristic frequencies of exciton transitions from the ground state to excited states^[21,22], and resonance effects connected with excitons and with the exciton condensate should appear in this band.

We have investigated free excitons in Ge at wavelengths 2000–500, 400–345, and 310–250 μ . To reduce the impurity contribution to the absorption and to the photoconductivity, we used Ge samples with total impurity concentration $N_d + N_a \lesssim 10^{12} \text{ cm}^{-3}$. The spectrum of the free excitons was investigated in the temperature range $T = 1.6\text{--}4.2^\circ \text{K}$ at an electron-hole pair optical generation level $10^{15}\text{--}10^{17} \text{ cm}^{-2} \text{ sec}^{-1}$. The exciton density n_e averaged over the sample did not exceed 10^{13} cm^{-3} (sample thickness $\sim 1 \text{ mm}$), and the spectra could be measured to $n_e = 10^{10} \text{ cm}^{-3}$. Absorption and photoconductivity lines due to free excitons was observed at 3.2–3.6 meV, and nonresonant photoconductivity due to the free excitons was observed in the interval 4–5 meV.

Figure 10 shows the absorption (a) and photoconductivity (b) spectra at $T = 1.6^\circ \text{K}$ and the photoconductivity spectrum (c) at $T = 4.2^\circ \text{K}$. The experiment was performed at $n_e \sim 10^{12} \text{ cm}^{-3}$. We see three well-resolved lines with energies 3.58, 3.42, and 3.3 meV, with a width $\sim 0.05 \text{ meV}$. The position of the lines in the absorption spectra and in photoconductivity is the same and does not depend on the temperature, while the relative intensities differ significantly. When the temperature is increased, the lines become broader. Either the photoconductivity or the absorption line intensity depends

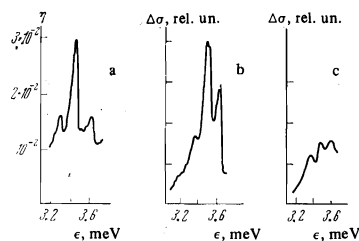


FIG. 10. a) Absorption spectrum of Ge with $N_d, N_a \approx 10^{12} \text{ cm}^{-3}$ (interband illumination, $T = 1.6^\circ \text{K}$, $n_e = 10^{12} \text{ cm}^{-3}$). b) Photoconductivity spectrum of Ge with $N_d, N_a \approx 10^{12} \text{ cm}^{-3}$ (interband illumination, $T = 1.6^\circ \text{K}$, $n_e = 10^{12} \text{ cm}^{-3}$). c) Photoconductivity spectrum of Ge with $N_d, N_a \approx 10^{12} \text{ cm}^{-3}$ (interband illumination, $T = 4.2^\circ \text{K}$, $n_e = 10^{12} \text{ cm}^{-3}$).

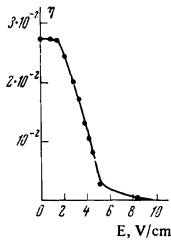


FIG. 11

FIG. 11. Dependence of the sample absorption coefficient $\eta = P_{\text{abs}}/P_{\text{inc}}$ (P is the radiation power) on the electric field (interband light, $T = 1.6^\circ\text{K}$, $n_e = 10^{12}\text{ cm}^{-3}$).

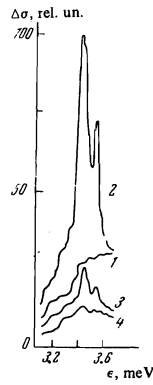


FIG. 12

FIG. 12. Photoconductivity spectra of Ge with $N_d, N_a < 10^{12}\text{ cm}^{-3}$ at different values of the bias (interband light, $T = 1.6^\circ\text{K}$, $n_e = 10^{12}\text{ cm}^{-3}$): 1) $E = 0.7\text{ V/cm}$, 2) $E = 3.5\text{ V/cm}$, 3) $E = 6.5\text{ V/cm}$, 4) $E = 10\text{ V/cm}$.

strongly on the electric field applied to the Ge sample. Figure 11 shows the dependence of the coefficient η of absorption of radiation by the sample on the electric field intensity E , plotted for a 3.42-meV line at $T = 1.6^\circ\text{K}$. Up to fields $E \approx 2\text{ V/cm}$, the absorption remains unchanged, and it decreases by approximately two orders of magnitude in the interval from 2 to 8 V/cm. Doubling the exciton concentration corresponds to $E = 3.5\text{ V/cm}$, which is in good agreement with the published data on impact ionization of excitons.^[23]

Figure 12 shows the photoconductivity spectra ($T = 1.6^\circ\text{K}$) at different values of E . We see that there are no exciton photoconductivity lines in weak electric fields ($E \lesssim 1\text{ V/cm}$), and when E is increased to 3.5 V/cm their intensity first increases strongly, and then decreases.

At $T = 4.2^\circ\text{K}$, the dependence of the line intensity on the electric field intensity E turns out to be weaker in the weak-field region, and remains the same as before in strong fields ($E \gtrsim 3.5\text{ V/cm}$). The nonresonant photoconductivity in the $\epsilon \sim 5\text{ meV}$ band is larger by approximately one order of magnitude than the resonant photoconductivity, and depends little on E at $E \lesssim 3\text{ V/cm}$ in the entire investigated temperature interval (1.6–4.2°K), but decreases rapidly at $E = 3.5\text{ V/cm}$.

An increase of the exciton concentration from 10^{10} to 10^{13} cm^{-3} does not lead to noticeable changes in the spectra, while the absorption of the radiation by the sample increases approximately linearly and reaches 15%. The results are the same if one varies not the optical-excitation levels, but the exciton lifetimes. The nonresonant conductivity depends little on the exciton concentration at $n_e \gtrsim 5 \times 10^{11}\text{ cm}^{-3}$, apparently as a result of the decrease of the free-carrier lifetime with increasing generation level.

Analysis of the experimental results shows that the observed lines correspond to transitions of free excitons from the ground state to excited states. Resonance photoconductivity is realized if the excitons excited by the submillimeter radiation dissociate under the influ-

ence of phonons or of the electric field. The nonresonant photoconductivity is apparently connected with photoionization of the free excitons.

The presented experimental results offer evidence of the new possibilities of investigating semiconductors with the aid of high-resolution spectroscopy at submillimeter wavelength. Obviously, the approach is far from limited to the problems considered in the present article.

- ¹M. B. Golant, R. L. Vilenskaya, E. A. Zylina, Z. F. Kaplun, A. A. Negirev, V. A. Parilov, T. B. Rebrova, and V. S. Savel'ev, *Prib. Tekh. Eksp.* No. 4, 136 (1965); M. B. Golant, Z. T. Alekseenko, Z. S. Korotkova, L. A. Lunkina, A. A. Negirev, O. P. Petrova, T. B. Rebrova, and V. S. Savel'ev, *ibid.* No. 3, 231 (1969).
- ²E. M. Gershenson and G. N. Gol'tsman, *ZhETF Pis. Red.* 14, 98 (1971) [*JETP Lett.* 14, 63 (1971)].
- ³G. N. Gol'tsman, *Prib. Tekh. Eksp.* No. 1, 136 (1972).
- ⁴W. Kohn, *Solid State Phys.* 5, 286, 1957.
- ⁵R. A. Faulkner, *Phys. Rev.* 184, 713, 1969.
- ⁶K. Calbow, *Canad. J. Phys.* 41, 1801, 1963.
- ⁷R. Barrier and K. Nishikawa, *Canad. J. Phys.* 41, 1823, 1963.
- ⁸J. H. Reuszer and P. Fisher, *Phys. Rev.* 135, A1125, 1964.
- ⁹T. M. Lifshitz and Ya. F. Nad', *Dokl. Akad. Nauk SSSR* 162, 801 (1965) [*Sov. Phys.-Doklady* 10, 532 (1965)].
- ¹⁰R. L. Jones and P. Fisher, *J. Phys. Chem. Sol.* 26, 1125, 1965.
- ¹¹R. Kaplan, M. A. Kinch and W. Scott, *Solid St. Comm.*, 7, 883, 1969.
- ¹²G. E. Stillman, C. M. Wolfe and J. O. Dimmock, *Sol. St. Comm.*, 7, 921, 1969.
- ¹³S. Narita and M. Miyao, *Sol. St. Comm.* 9, 2161, 1971.
- ¹⁴E. M. Gershenson, G. N. Gol'tsman and N. G. Ptitsina, *Fiz. Tekh. Poluprov.* [*Sov. Phys.-Semicond.* 7 (1973) (in print)].
- ¹⁵J. Nisida and K. Norii, *J. Phys. Soc. Japan* 26, 388, 1969.
- ¹⁶K. Norii and J. Nisida, *J. Phys. Soc. Japan* 31, 783, 1971.
- ¹⁷E. M. Gershenson and G. N. Gol'tsman, *Fiz. Tekh. Poluprov* 6, 580 (1972) [*Sov. Phys.-Semicond.* 6, 509 (1972)].
- ¹⁸E. M. Gershenson, G. N. Gol'tsman, V. V. Emtsev, T. V. Mashovets, N. G. Ptitsina, and S. M. Ryvkin, *ZhETF Pis. Red.* 14, 360 (1971) [*JETP Lett.* 14, 241 (1971)].
- ¹⁹E. M. Gershenson, G. N. Gol'tsman, and A. P. Mel'nikov, *ZhETF Pis. Red.* 14, 281 (1971) [*JETP Lett.* 14, 185 (1971)].
- ²⁰M. A. Lampert, *Phys. Rev. Lett.* 1, 450, 1958.
- ²¹E. F. Gross, S. A. Permogorov, and B. S. Razbirin, *Usp. Fiz. Nauk* 103, 431 (1971) [*Sov. Phys.-Uspekhi* 14, 104 (1971)].
- ²²E. M. Gershenson, G. N. Gol'tsman, and N. G. Ptitsina, *ZhETF Pis. Red.* 16, 228 (1972) [*JETP Lett.* 16, 161 (1972)].
- ²³A. A. Rogachev and S. M. Ryvkin, *Fiz. Tekh. Poluprov.* 1, 1740 [*Sov. Phys.-Semicond.* 1, 1445 (1968)].

Translated by J. G. Adashko

65